

---

This is the **accepted version** of the journal article:

Jiménez, Rafael; Pequerul, Raquel; Amor Minguez, Adrián; [et al.]. «Inhibitors of aldehyde dehydrogenases of the 1A subfamily as putative anticancer agents : Kinetic characterization and effect on human cancer cells». *Chemico-Biological Interactions*, Vol. 306 (2019), p. 123-130. 8 pàg. DOI 10.1016/j.cbi.2019.04.004

---

This version is available at <https://ddd.uab.cat/record/288518>

under the terms of the  <sup>IN</sup>  
COPYRIGHT license


---

This is the **accepted version** of the journal article:

Jiménez, Rafael; Pequerul, Raquel; Amor Minguez, Adrián; [et al.]. «Inhibitors of aldehyde dehydrogenases of the 1A subfamily as putative anticancer agents : Kinetic characterization and effect on human cancer cells». *Chemico-Biological Interactions*, Vol. 306 (2019), p. 123-130. 8 pàg. DOI 10.1016/j.cbi.2019.04.004

---

This version is available at <https://ddd.uab.cat/record/288518>

under the terms of the  **IN** COPYRIGHT license

# Inhibitors of aldehyde dehydrogenases of the 1A subfamily as putative anticancer agents: kinetic characterization and effect on human cancer cells

**Rafael Jiménez<sup>1</sup>, Raquel Pequerul<sup>1</sup>, Adrián Amor<sup>1</sup>, Julia Lorenzo<sup>1,2</sup>, Kamel Metwally<sup>3</sup>,  
Francesc Xavier Avilés<sup>1,2</sup>, Xavier Parés<sup>1</sup>, Jaume Farrés<sup>1</sup>**

<sup>1</sup>Department of Biochemistry and Molecular Biology, Faculty of Biosciences, Universitat Autònoma de Barcelona, E-08193 Bellaterra (Barcelona), Spain.

<sup>2</sup>Institute for Biotechnology and Biomedicine, Universitat Autònoma de Barcelona, E-08193 Bellaterra (Barcelona), Spain.

<sup>3</sup>Department of Medicinal Chemistry, Faculty of Pharmacy, Zagazig University, Zagazig, Egypt.

---

## ABSTRACT

Aldehyde dehydrogenases (ALDHs) are enzymes catalyzing the NAD(P)<sup>+</sup>-dependent oxidation of aldehydes to their corresponding carboxylic acids. High ALDH activity has been related to some important features of cancer stem cells. ALDH1A enzymes, involved in the retinoic acid signaling pathway, are promising drug targets for cancer therapy, and the design of selective ALDH1A inhibitors has a growing pharmacological interest. In the present work, two already known compounds (DEAB and WIN 18,446) and novel thiazolidinedione and pyrimidoquinoline acetic acid derivatives (compounds **5a** and **64**, formerly described as aldo-keto reductase inhibitors) were tested as inhibitors of the ALDH1A enzymes (namely, ALDH1A1, ALDH1A2 and ALDH1A3) as a first step to develop some potential drugs for cancer therapy. The inhibitory capacity of these compounds against the ALDH1A activity was characterized *in vitro* by using purified recombinant proteins. The IC<sub>50</sub> values of each compound were determined indicating that the most potent inhibitors against ALDH1A1, ALDH1A2 and

ALDH1A3 were DEAB, WIN 18,446 and compound **64**, respectively. Type of inhibition and  $K_i$  values were determined for DEAB against ALDH1A1 (competitive,  $K_i = 0.13 \mu\text{M}$ ) and compound **64** against ALDH1A3 (non-competitive,  $K_i = 1.77 \mu\text{M}$ ). The effect of these inhibitors on A549 human lung cancer cell viability was assessed, being compound **64** the only inhibitor showing an important reduction of cell survival. We also tested the effect of the ALDH substrate, retinaldehyde, which was cytotoxic above  $10 \mu\text{M}$ . This toxicity was enhanced in the presence of DEAB. Both DEAB and compound **64** were able to inhibit the ALDH1A activity in A549 cells. The current work suggests that, by blocking ALDH activity, drug inactivation may be avoided. Thus these results may be relevant to design novel combination therapies to fight cancer cell chemoresistance, using both enzyme inhibitors and chemotherapeutic agents.

### Highlights

- Four compounds were tested *in vitro* and *in cellula* as inhibitors of ALDH1A enzymes
- DEAB was a selective and competitive ALDH1A1 inhibitor in the nanomolar range
- WIN 18,446 was a selective and irreversible ALDH1A2 inhibitor
- A thiazolidinedione derivative was the most potent non-competitive ALDH1A3 inhibitor
- Retinaldehyde had a toxic effect on A549 cells which was enhanced by DEAB cotreatment

### Keywords

Aldehyde dehydrogenase; Cancer; Cancer stem cell; Enzyme inhibitor; Retinaldehyde; Retinoic acid

## 1. Introduction

Cancer is one of the leading causes of morbidity and mortality worldwide. According to the World Health Organization (WHO), it is currently the second leading cause of death globally, and its incidence is expected to rise significantly over the following decades [1]. Current therapies against cancer are mainly based on the so-called stochastic model of cancer development, which assumes that, although cell population within a tumor is heterogeneous, all cells have an equal likelihood of acquiring mutations and initiating a tumor [2]. These therapies, consisting of surgery, chemotherapy and radiotherapy, are unspecific, leading to toxic side effects on healthy cells, directly impairing the patient's life quality.

Since current therapies are usually not fully effective in curing cancer, another model, called hierarchical model, has gained relevance. According to this model, some specific cells within the tumor, the so-called cancer stem cells (CSCs), are the responsible for the initiation and maintenance of the tumor, and also for relapse of a more aggressive and resistant cancer [3]. Therapies based on the hierarchical model aim to target CSCs specifically, and thus, the discovery of markers specific for CSCs can be crucial for the development of new treatments against cancer. Recently, the increased aldehyde dehydrogenase (ALDH) activity has been evidenced as a marker for the identification of CSCs. The high expression of ALDH activity in this subpopulation of cells has been observed in many cancers, including lung, breast, colon, prostate, bladder, brain, melanoma and cervical, among others [4].

ALDHs catalyze the  $\text{NAD(P)}^+$ -dependent irreversible oxidation of a wide range of endogenous and exogenous aldehydes to their corresponding carboxylic acids. Their ability to perform this reaction makes ALDHs crucial for the cellular protection against aldehydes, highly reactive compounds that are often cytotoxic and carcinogenic [5]. Furthermore, some ALDH forms, such as the cytosolic enzymes ALDH1A1, ALDH1A2 and ALDH1A3 (which will be studied in the present work), play important roles in cell signaling via oxidation of retinaldehyde to retinoic acid. In the cell, retinoic acid produced in the cytoplasm binds to cellular retinoic acid binding protein type II, and is transferred to the nucleus where it binds to heterodimers of retinoic acid

receptor (RAR) and retinoid X receptor (RXR). Once activated, these receptor complexes bind to retinoic acid response elements (RAREs), which are regulatory sequences that induce gene transcription and modulate a wide range of biological processes, including cell proliferation, differentiation, cell cycle arrest and apoptosis [4].

The role of the increased ALDH activity in CSCs is not well understood yet. Nevertheless, the “stemness” characteristics of this subpopulation of cells have been particularly related to the participation of ALDHs in retinoic acid-mediated signaling pathways, and also to the high antioxidant activity of these enzymes, specifically their ability to reduce reactive oxygen species (ROS) [6]. This ability to scavenge ROS has been attributed to the resistance of CSCs against radiation and some anti-neoplastic agents. In fact, ALDHs have been shown to metabolize some prominent drugs, such as cyclophosphamide, paclitaxel and doxorubicin, into non-toxic forms [3].

Therefore, the inhibition of ALDHs could be a promising new approach to fight cancer, especially the inhibition of the forms involved in retinoic acid signaling, namely ALDH1A1, ALDH1A2 and ALDH1A3. It should be taken into account that, although ALDH activity has been defined as a marker for CSCs, at the protein level, the ALDH form responsible for the activity is cancer-specific [4]. Thus, it is of interest to identify the active ALDH forms for specific cancers, and also to discover form-selective inhibitors as potential chemotherapeutic agents for each type of cancer. Several inhibitors of ALDHs have been reviewed recently [7], but unfortunately there are not many specific inhibitors currently used in clinical trials [3]. Although ALDH enzymes share similarities in structure and function, as well as some overlap in substrate preferences, each of the enzymes has evolved different aldehyde binding sites (and thus, distinct substrate specificities) [8]. Taking advantage of these differences in the active-site architecture would allow for the design of new inhibitors selective for each enzyme.

In view of the promising possibilities of targeting ALDHs for cancer treatment, the objective of this work was to characterize four different synthetic compounds, namely N,N-diethylaminobenzaldehyde (DEAB), compound **5a**, WIN 18,446 and compound **64**, as

putative ALDH1A inhibitors, and test their efficacy as potential drugs for anticancer therapy. First, the compounds were characterized as inhibitors against the cytosolic enzymes ALDH1A1, ALDH1A2 and ALDH1A3 by determining the half-maximal inhibitory concentration ( $IC_{50}$ ), the type of inhibition and the inhibition constant ( $K_i$ ) value. Then, studies on A549 human lung cancer cells were carried out, specifically to determine the expression pattern of ALDH1A enzymes in these cells, the effect of the inhibitors on cell viability and the cellular ALDH activity in the absence or presence of inhibitor.

## 2. Materials and methods

### 2.1. Compounds tested

Four different synthetic compounds were tested in this study (**Figure 1**): **(A)** DEAB (N,N-diethylaminobenzaldehyde, obtained from Sigma Aldrich), **(C)** WIN 18,446 (N,N'-(octane-1,8-diyl)bis(2,2-dichloroacetamide), obtained from Cayman Chemical), and compounds **(B)** **5a** (a 2,4-thiazolidinedione-3-acetic acid derivative) and **(D)** **64** (a 1-oxopyrimido[4,5-*c*]quinoline-2-acetic acid derivative), synthesized as described previously [9,10].

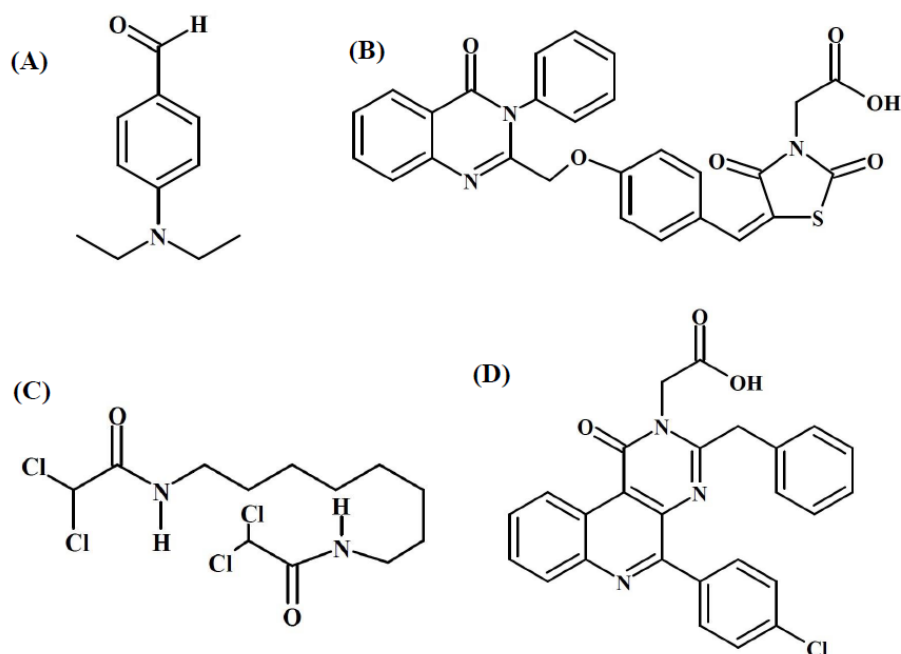


**Figure 1.** Molecular structure of the compounds tested as putative inhibitors of ALDH activity and as potential anticancer agents. **(A)** DEAB, **(B)** compound **5a**, **(C)** WIN 18,446, **(D)** compound **64**. (Single column fitting image).

## 2.2. Cell culture

The cell lines used in the study were A549 (human lung cancer), HL-60 (human acute promyelocytic leukemia), K-562 (human chronic myelogenous leukemia) and A-431 (human epidermoid carcinoma), all obtained from the American Type Culture Collection (ATCC). A549 and A-431 cells were maintained in DMEM (Dulbecco's Modified Eagle Medium, Life Technologies) supplemented with 10% FBS (Fetal Bovine Serum, Life Technologies), at 37°C and 10% CO<sub>2</sub> in air. HL-60 and K-562 cells were maintained in RPMI (Roswell Park Memorial Institute, Life Technologies) medium supplemented with 10% FBS, 1% sodium pyruvate (Invitrogen) and 1% non-essential amino acids (Invitrogen), at 37°C and 5% CO<sub>2</sub> in air.

## 2.3. Protein expression and purification

Human ALDH1A1, ALDH1A2 and ALDH1A3 were expressed from the pET-30 Xa/LIC constructs in transformed *E. coli* BL21(DE3)pLys cells and affinity purified onto a Ni<sup>2+</sup>-NTA Chelating Sepharose™ Fast Flow column (GE Healthcare) as previously described [11].

## 2.4. Fluorimetric activity assays

In order to determine the IC<sub>50</sub> values, reaction rates were determined at various concentrations of inhibitor at fixed saturating substrate concentrations. Hexanal (Sigma) was used as the substrate for all the reactions, at 5 μM for ALDH1A1, and 250 μM for ALDH1A2 and ALDH1A3. Reactions were monitored using a Cary Eclipse (Varian) fluorimeter at 25°C. All reactions were performed in quartz cuvettes in a final volume of 1 mL, in the presence of 1% DMSO (Sigma) and 0.5 mM NAD<sup>+</sup> cofactor (Apollo Scientific). Fluorescence of NADH was followed at 460 nm with excitation at 340 nm and spectral bandwidth of 10 nm. The reaction



mixture also contained 5  $\mu$ M NADH (Apollo Scientific) as an internal standard to obtain absolute reaction rates, which were calculated according to the equation:  $v = \frac{dF}{dt} \frac{C_{st}}{F_{st}}$ , where  $C_{st}$  is the standard NADH concentration,  $F_{st}$  the standard fluorescence and  $dF/dt$  the slope of the time dependent fluorescence [12]. In all cases, specific activity was expressed in units (U)/mg, one unit being defined as 1  $\mu$ mol of product formed per min. ALDH1A1 and ALDH1A2 were assayed in 50 mM HEPES (Sigma), 0.5 mM EDTA, 0.5 mM DTT, pH 8.0, while ALDH1A3 assays were performed in 50 mM HEPES, 30 mM MgCl<sub>2</sub>, 5 mM DTT, pH 8.0. The IC<sub>50</sub> values were calculated by nonlinear fitting of the obtained data to a sigmoidal plot using GraFit 5.0 (Erithacus software), with the following 4-parameter equation:  $y = \frac{range}{1 + (\frac{x}{IC_{50}})^s} + background$ ,

where  $y$  is the specific activity,  $x$  is the inhibitor concentration, *background* is the minimum  $y$  value, *range* is the fitted uninhibited value minus the background, and  $s$  is a slope factor. Values were expressed as the mean  $\pm$  SE.

Activity assays to determine the type of inhibition and K<sub>i</sub> value were performed using various substrate concentrations at fixed inhibitor concentrations (from 0.1x to 10x IC<sub>50</sub>), maintaining the same conditions of the IC<sub>50</sub> experiments and using GraFit 5.0 for data processing. The data of enzymatic activities at different inhibitor concentrations were fitted to the Michaelis-Menten equation to determine the values of K<sub>m</sub> and V<sub>max</sub>. Then, results were fitted to the equations of the different types of enzymatic inhibition and K<sub>i</sub> values were determined choosing the type of inhibition yielding the best fit. Values were expressed as the mean  $\pm$  SE.

## 2.5. Immunoassays

Western blotting was performed in order to assess the expression of the different ALDH1A enzymes in A549 cells. Previously, extraction of proteins was achieved by solubilizing the cell pellets in 200-500  $\mu$ L of M-PER reagent (Mammalian Protein Extraction Reagent, Thermo Scientific), depending on the size of the pellet. Cell debris was eliminated by centrifugation at 14,000 x g for 10 min and the total protein content of the supernatant was determined by the

Bradford method. Then, 20 µg of protein of each cell line was loaded on an SDS-PAGE gel (in the case of A549 cells, 0.5 µg for the ALDH1A1 assay and 5 µg for the ALDH1A3 assay). After the electrophoretic analysis, protein was transferred to a PVDF membrane (Merck Millipore) in transfer buffer (10% Tris-Gly, pH 8.0, 10% methanol). After the transfer, the membrane was washed with phosphate-buffered saline (10 mM sodium hydrogen phosphate, 1.8 mM potassium dihydrogen phosphate, 137 mM sodium chloride, 2.7 mM potassium chloride, pH 7.4, PBS)-0.05% Tween 20 solution and blocked with a solution of 5% skimmed milk in PBS-0.05% Tween 20. Then, the membrane was washed again with PBS-0.05% Tween 20 and incubated overnight at 4°C with primary antibodies specific against ALDH1A1, ALDH1A2 or ALDH1A3 diluted in PBS-0.05% Tween 20 with 2% skimmed milk (**Supplementary Table S1**). After washing with PBS-0.05% Tween 20 solution, the membrane was incubated with peroxidase-conjugated secondary polyclonal antibodies specific against mouse or rabbit antibody constant fraction (diluted in PBS-0.05% Tween 20 with 2% skimmed milk solution), at room temperature. After washing again, detection of the enzymes on the membrane was possible using a Western horseradish peroxidase (HRP) substrate (Luminata<sup>TM</sup> Classico, Merck Millipore) and Quantity One software.

## *2.6. Cytotoxicity assays*

The effect of the different inhibitors was tested by using the PrestoBlue<sup>TM</sup> Cell Viability Reagent (Invitrogen) on A549 cells. Cells ( $2 \cdot 10^3$  per well) were seeded on 96-well plates in a final volume of 100 µL of culture medium and incubated at 37°C and 10% CO<sub>2</sub> in air, overnight, in order to allow cells adhere to the wells. On the other hand, dilutions of the inhibitor were prepared in growth medium from a 50 mM stock of inhibitor in DMSO. Then, 100 µL of the corresponding dilution of inhibitor were added to the cells, to final concentrations of inhibitor of 0, 1, 5, 10, 25, 50, 100 and 200 µM. After 24 or 72 h of incubation, 10 µL of the PrestoBlue<sup>TM</sup> reagent were added to each well and, after 3 h, fluorescence was read in a Perkin Elmer Victor 3 Multilabel Plate Reader (excitation wavelength at 531 nm and emission wavelength at 572 nm). Comparison of arbitrary units of fluorescence of the wells without

inhibitor with those with inhibitor allowed the determination of the percentage of cell viability at each inhibitor concentration. Three independent experiments run in triplicate were performed. Data were represented as the mean  $\pm$  SE of triplicates from a single representative experiment. Student's *t*-test (R software) was performed to establish significance between groups. The significance level was set at  $p < 0.05$ .

In addition, the toxic effect of retinaldehyde was tested on A549 cells in the absence or presence of 100  $\mu$ M DEAB. Dilutions of all-*trans*-retinaldehyde (Sigma) in medium were prepared from a concentrated stock in ethanol, and added to the plate to final concentrations of 0, 10, 20, 30, 40, 50 and 60  $\mu$ M, not exceeding 0.5% (v/v) ethanol final concentration. These assays were performed as described above, but under dim red light to avoid the photoisomerization of retinoid double bonds.

## *2.7. Cellular enzymatic activity assays with retinoids*

Retinaldehyde dehydrogenase activity was determined in A549 cells using an optimized HPLC-based method, as follows. Two-hundred thousand cells per well were seeded in a final volume of 1.5 mL on 6-well plates and incubated at 37°C and 10% CO<sub>2</sub> in air, overnight. After incubation, a concentrated stock of retinaldehyde in ethanol was diluted in cell growth medium and added to the corresponding wells at a final concentration of 30  $\mu$ M, never exceeding 0.5% (v/v) ethanol in the culture media. In the control plate, ethanol (diluted in growth medium) was added instead of retinaldehyde. Dilutions of stocks of inhibitor in 1% DMSO were prepared in growth medium and added to the wells. Medium and cells were recovered separately after incubation at 37°C for 1 h or 5 h (only 1 h when inhibitor was added) and kept in an ice bath. Cells were obtained by trypsinization of the culture and centrifugation, and then were lysed by adding PBS with 1% SDS and sonication in cold water for 10 min. Lysed cells were then centrifuged at 16,110  $\times$  g for 15 min. Media aliquots (500  $\mu$ L) and cell extracts were added to disposable glass tubes and 30- $\mu$ L aliquots of cell extracts were collected to quantify total protein content by using a Bradford assay method. To perform retinoid extraction, 100  $\mu$ L of 2.5 M

ammonium acetate, pH 4.5, was added in order to acidify the aqueous phase and facilitate the retinoic acid recovery [13]. Then, 1 mL of cold methanol and 2 mL of hexane were added twice, and samples were vortex mixed and centrifuged at 16,110 x g for 1 min. Samples were then treated as previously described [11]. Elution was monitored at 370 nm for all-*trans*-retinaldehyde and 350 nm for all-*trans*-retinoic acid, using a Waters 2996 photodiode array detector. Quantification of retinoids was performed by interpolating HPLC peak areas into a calibration curve and specific ALDH activity was calculated taking into account the protein amount quantified in cell extracts by the Bradford assay and the amount of retinoic acid produced. Specific activity was expressed in U/mg of total protein, being 1 U equal to 1  $\mu$ mol of product formed per min.

### 3. Results and discussion

#### 3.1. *In vitro* characterization of the inhibitors with recombinant enzymes

The IC<sub>50</sub> values of each compound for each ALDH1A enzyme are shown in **Table 1**. Sigmoidal plots resulting from the inhibition of the enzymes are presented in the **Supplementary Figures S1 to S4**.

**Table 1.** IC<sub>50</sub> values of each compound against ALDH1A enzymes. (Single column fitting table)

Enzyme	IC <sub>50</sub> ( $\mu$ M)			
	DEAB	compound 5a	WIN 18,446	compound 64
ALDH1A1	0.18 $\pm$ 0.05	5.4 $\pm$ 0.5	56 $\pm$ 2	NI
ALDH1A2	9.5 $\pm$ 3.2	NI	0.07 $\pm$ 0.01	3.5 $\pm$ 0.8
ALDH1A3	47 $\pm$ 17	23 $\pm$ 4	31 $\pm$ 8	1.2 $\pm$ 0.1

Hexanal was used as the substrate. IC<sub>50</sub> values were the mean  $\pm$  SE resulting from duplicate experiments. NI: no inhibition was observed.

For DEAB, the lowest value of IC<sub>50</sub> is obtained against ALDH1A1, being in the nanomolar range. This compound is a less potent inhibitor for ALDH1A2 and ALDH1A3. These results are in good agreement with those obtained by Morgan *et al.* [14], who also found that the most potent inhibition with DEAB was achieved against ALDH1A1, followed by ALDH1A2 and ALDH1A3. However, they calculated an IC<sub>50</sub> value against ALDH1A1 of 57 nM, using propionaldehyde as the substrate of the reaction. The IC<sub>50</sub> value for an inhibitor depends on the relative substrate concentration (i.e., on the ratio substrate concentration/K<sub>m</sub>) when the inhibition is competitive. This may account for the slightly higher IC<sub>50</sub> values reported in the present work, determined at a relatively higher substrate concentration

Compound **5a**, previously described as an aldo-keto reductase inhibitor [9], is also a good inhibitor against ALDH1A1, but it is not as potent as DEAB.

The IC<sub>50</sub> value for WIN 18,446 *versus* ALDH1A2 is quite low, in the nanomolar range, indicating that this compound is an excellent inhibitor of this enzyme. Conversely, it is neither a potent inhibitor of ALDH1A1 nor ALDH1A3. WIN 18,446 has been previously described as an irreversible inhibitor of ALDH1A2 [15], thus it is not surprising that the IC<sub>50</sub> value obtained against ALDH1A2 is that low. Chen *et al.* [16] observed a time-dependent inhibition of ALDH1A2 by WIN 18,446, with an apparent IC<sub>50</sub> value of 0.19  $\mu$ M upon 22 min of pre-incubation. We obtained an IC<sub>50</sub> value of 0.07  $\mu$ M using an incubation time of 5 min.

Finally, compound **64** is efficient at inhibiting ALDH1A2 and ALDH1A3, especially the latter. Like compound **5a**, compound **64** has been recently described as an aldo-keto reductase inhibitor [10]; here, its ability to inhibit ALDHs is evidenced. Although compound **64** is not selective for ALDH1A3, the fact that we obtained such a low IC<sub>50</sub> value is promising, since few potent inhibitors of ALDH1A3 have been found so far.

The type of inhibition and  $K_i$  value were determined only for the best inhibitor compounds (**Table 1**). Since WIN 18,446 had already been described as an irreversible inhibitor of ALDH1A2, the experiments were only carried out for DEAB against ALDH1A1 and compound **64** against ALDH1A3. To this end, global fitting of the data to the different types of enzymatic inhibition was performed. Data plotted to the best fitting type of inhibition are shown in **Figure 2** for DEAB, and in **Figure 3** for compound **64**. Data fitted to the other types of enzymatic inhibition are not shown here. In addition, **Supplementary Figures S5** and **S6** show the individual fittings of the data at each inhibitor concentration to the Michaelis-Menten equation.

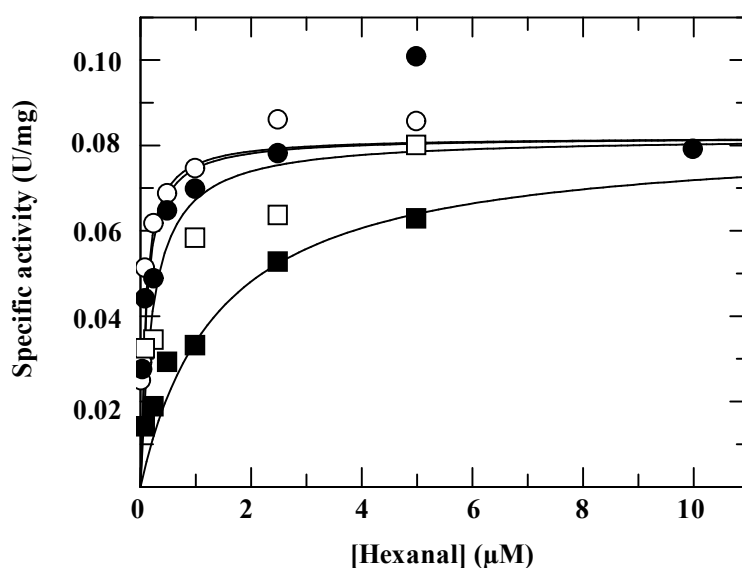


**Figure 2.** Competitive fit of DEAB inhibition against ALDH1A1 at various concentrations of DEAB. —○— 0  $\mu\text{M}$ ; —●— 0.02  $\mu\text{M}$ ; —□— 0.2  $\mu\text{M}$ ; —■— 2  $\mu\text{M}$ . Hexanal was used as the substrate of the reaction. The values of the kinetic parameters calculated from this fit were:  $V_{\max} = 0.082 \pm 0.003$  U/mg;  $K_m = 0.086 \pm 0.016$   $\mu\text{M}$ ;  $K_i = 0.130 \pm 0.034$   $\mu\text{M}$ . Data are the mean of duplicate experiments. (Single column fitting image)

Data for DEAB against ALDH1A1 are shown in **Figure 2** and were fitted to the equation for competitive inhibition, given by  $v = \frac{V_{\max}[S]}{[S] + K_m(1 + \frac{[I]}{K_i})}$ , as described in [17]. In the study carried out by Morgan *et al.* [14], the authors also concluded that DEAB was a competitive inhibitor of ALDH1A1. This is further supported by the information given by the individual Michaelis-

Menten plots (**Supplementary Figure S5**), where it can be observed that, in the presence of DEAB, the  $K_m$  value tends to increase with increasing concentration of DEAB, whereas the  $V_{max}$  value barely changes. The calculated value for  $K_i$  was  $0.130 \pm 0.034 \mu\text{M}$ , which indicates that DEAB is an excellent inhibitor for ALDH1A1.

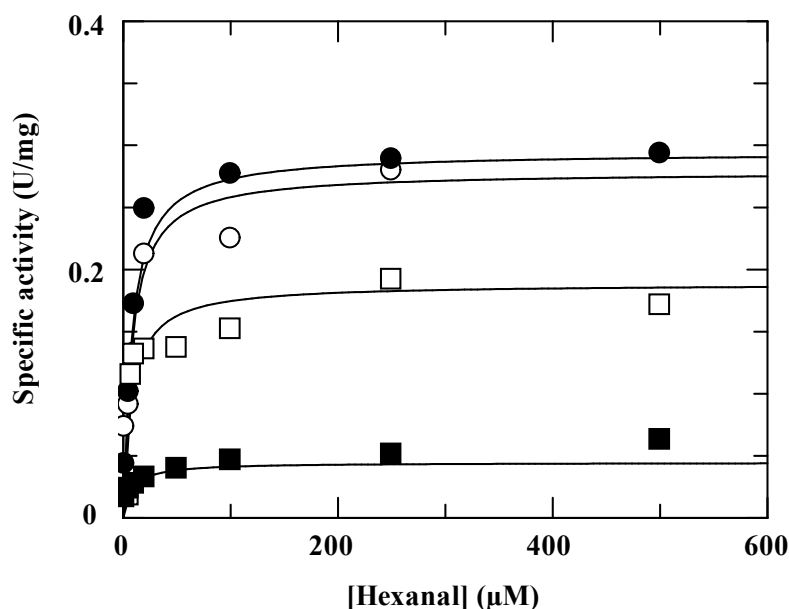


**Figure 3.** Non-competitive fit of compound **64** inhibition against ALDH1A3 at various concentrations of compound **64**. —○— 0  $\mu\text{M}$ ; —●— 0.1  $\mu\text{M}$ ; —□— 1  $\mu\text{M}$ ; —■— 10  $\mu\text{M}$ . Hexanal was used as the substrate of the reaction. The values of the kinetic parameters calculated from this fit were:  $V_{max} = 0.30 \pm 0.01 \text{ U/mg}$ ;  $K_m = 8 \pm 1 \mu\text{M}$ ;  $K_i = 1.77 \pm 0.32 \mu\text{M}$ . Data are the mean of duplicate experiments. (Single column fitting image)

Data for compound **64** against ALDH1A3 is shown in **Figure 3** and were fitted to the equation for non-competitive inhibition, given by  $v = \frac{V_{max} \cdot [S]}{([S] + K_m) \cdot (1 + \frac{[I]}{K_i})}$ , as described in [17]. Information provided by the individual Michaelis-Menten plots (**Supplementary Figure S6**) also suggests that compound **64** is a non-competitive inhibitor of ALDH1A3, since in the presence of the compound the  $K_m$  value remains approximately the same at different concentrations of inhibitor, whereas the  $V_{max}$  value is decreased at higher concentrations. The calculated value for  $K_i$  was  $1.77 \pm 0.32 \mu\text{M}$ , showing that compound **64** is a really suitable inhibitor of ALDH1A3.

Type of inhibition and  $K_i$  values for the best inhibitors against each ALDH1A enzyme are summarized in **Table 2**.

**Table 2.** Type of inhibition and  $K_i$  values of DEAB, WIN 18,446 and compound **64** against ALDH1A enzymes. (Single column fitting table)

Inhibitor	Most inhibited enzyme	Type of inhibition	$K_i$ ( $\mu$ M)
DEAB	ALDH1A1	Competitive	$0.130 \pm 0.034$
WIN 18,446	ALDH1A2	Irreversible <sup>a</sup>	—
<b>64</b>	ALDH1A3	Non-competitive	$1.77 \pm 0.32$

The type of inhibition and mean  $K_i$  values  $\pm$  SE, resulting from duplicate experiments, are indicated for the compounds showing the highest inhibitory potency against each ALDH1A enzyme, based on the  $IC_{50}$  results. <sup>a</sup>Result taken from Ref. [15].

### 3.2. Studies on human cancer cell lines

#### 3.2.1. Expression pattern of ALDH1A enzymes

The expression of each cytosolic ALDH1A enzyme was assessed on A549 lung cancer cells by Western blotting. A549 cells have already been known to express only ALDH1A1 and ALDH1A3 [18], but it was important to confirm this point in order to be able to discuss the subsequent experiments on these cells. Results are shown in **Figure 4**.



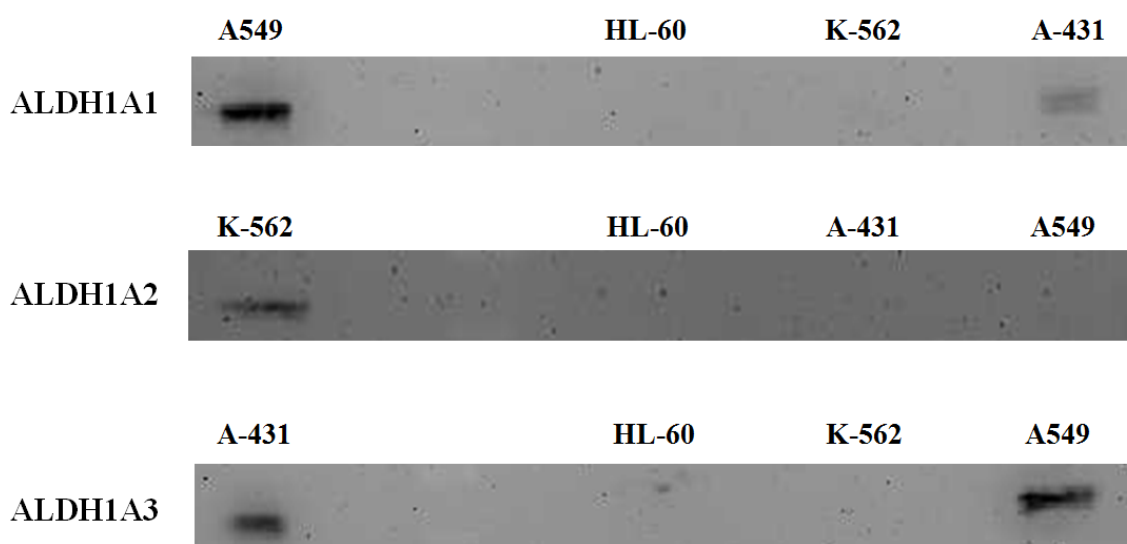


**Figure 4.** Western blot analysis of the expression of ALDH1A enzymes in human cancer cell lines. HL-60 cells were used as a negative control for the three enzymes. K-562 and A-431 cells were used as positive controls for ALDH1A2 and ALDH1A3, respectively. (2-column fitting image)

These results suggest that, indeed, A549 cells express high levels of both ALDH1A1 and ALDH1A3, but do not express ALDH1A2.

### 3.2.2. Cytotoxicity of the analyzed compounds and retinaldehyde on A549 cells

The toxicity of the four previously characterized inhibitors was evaluated on A549 cells. The results are presented in **Figures 5 to 8**.

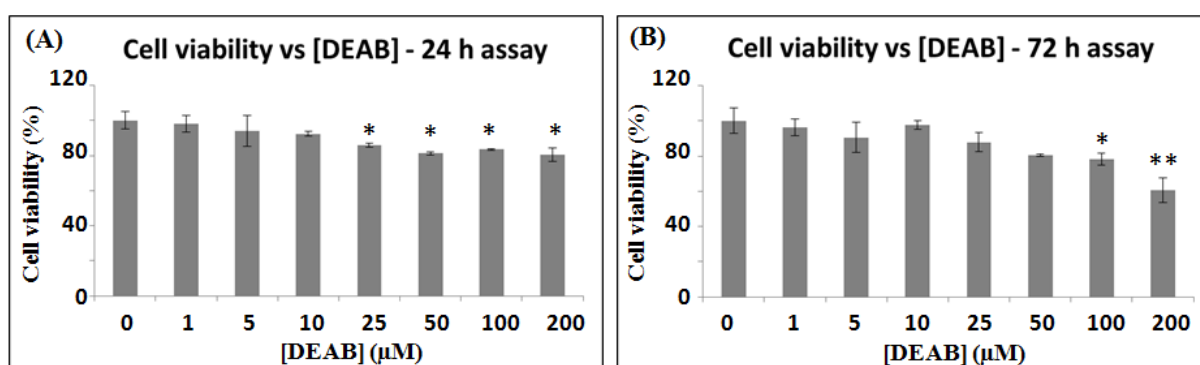


**Figure 5.** Bar diagram of A549 cell viability assays after treatment with DEAB for (A) 24 h and (B) 72 h.

Data are the mean  $\pm$  SE of percentage values relative to untreated controls ( $n = 3$ ) from a single

representative experiment.  $*p < 0.05$ ,  $**p < 0.01$ , compared with untreated controls. (2-column fitting image)

As shown in **Figure 5**, cell viability decreases when the concentration of DEAB is increased. Specifically, cell viability is decreased down to approximately 80 and 60% at the highest concentration of DEAB (200  $\mu\text{M}$ ), after 24 h and 72 h of incubation, respectively. These results are similar to those obtained by Park *et al.* [18], who also tested the effect of DEAB on A549 cells.

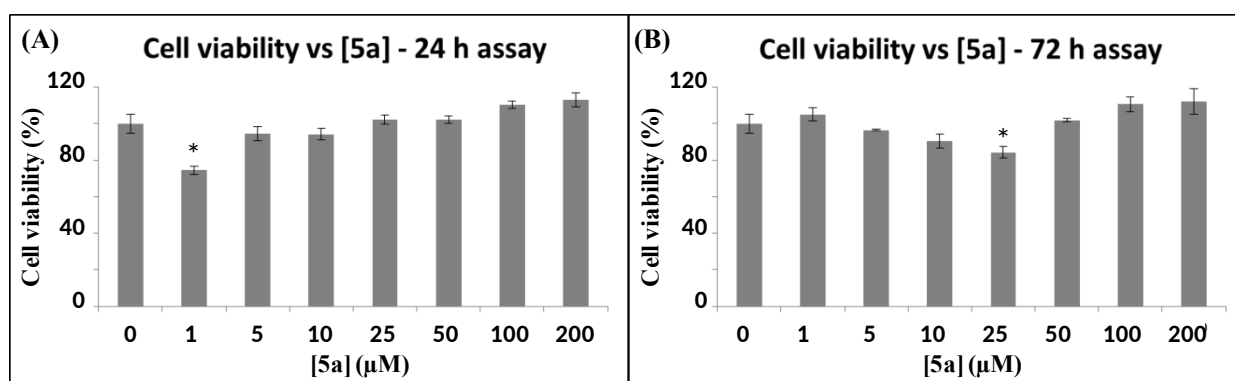


**Figure 6.** Bar diagram of A549 cell viability assays after treatment with compound **5a** for (A) 24 h and (B) 72 h. Data are the mean  $\pm$  SE of percentage values relative to untreated controls ( $n = 3$ ) from a single representative experiment.  $*p < 0.05$ , compared with untreated controls. (2-column fitting image)

**Figure 6** shows the results for compound **5a**. In this case, cell viability does not decrease as the concentration of inhibitor is increased. Similar results are obtained regardless of the time of incubation with the inhibitor.

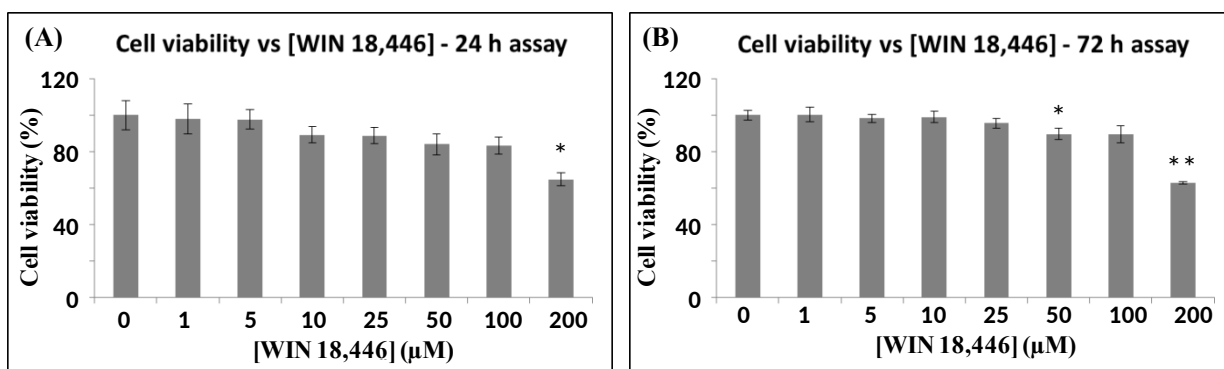


**Figure 7.** Bar diagram of A549 cell viability assays after treatment with WIN 18,446 for (A) 24 h and (B) 72 h. Data are the mean  $\pm$  SE of percentage values relative to untreated controls (n =3) from a single representative experiment. \* $p$  < 0.05, \*\* $p$  < 0.01, compared with untreated controls. (2-column fitting image)

It can be observed in **Figure 7** that WIN 18,446 has a similar effect on A549 cells to that of DEAB: cell viability decreases as the concentration of inhibitor increases. The results are similar at incubation times of 24 and 72 h.

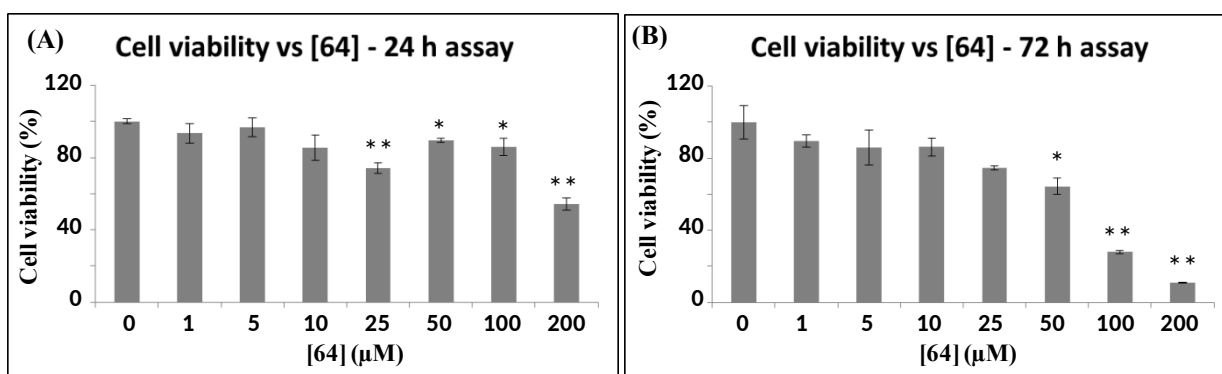


**Figure 8.** Bar diagram of A549 cell viability assays after treatment with compound **64** for (A) 24 h and (B) 72 h. Data are the mean  $\pm$  SE of percentage values relative to untreated controls (n = 3) from a single representative experiment. \* $p$  < 0.05, \*\* $p$  < 0.01, compared with untreated controls. (2-column fitting image)

Results of cytotoxicity assays with compound **64**, represented in **Figure 8**, yielded a similar pattern to those with DEAB and WIN 18,446. Cell survival was also reduced with increasing inhibitor concentration, but in this case, some differences could be observed between the assays at 24 and 72 h. At 24 h, cell viability was decreased down to 50% at 200  $\mu$ M compound **64**, whereas at 72 h the toxic effect of the inhibitor was evident at lower concentrations. At 200  $\mu$ M compound **64**, cell survival decreased down to 10%.

To sum up, compound **5a** is the only compound that does not seem to have any toxic effect on A549 cells. This may be due to the fact that compound **5a** is a quite large molecule that may not be easily internalized by the cells. Conversely, incubation with the other tested compounds

(which, in fact, are smaller), resulted in a reduction of cell viability at high concentrations of inhibitor. Specifically, compound **64** was the most potent compound at reducing cell viability, especially when incubated for 72 h. Compound **64** is also a large molecule, and cells may need more time to fully uptake this compound, thus the toxic effect cannot be completely seen at 24 h. Smaller molecules, such as DEAB and WIN 18,446, probably diffuse rapidly through the cell membrane, and thus no differences are appreciable after 24- and 72-h incubation.

Regardless of the size of the compounds, toxicity or lack of toxicity may be also associated to the intrinsic properties of each compound and their effects inside the cell. Once a given compound enters the cell, its toxicity can be the result of the inhibition of ALDH activity by the compound, or it may be produced by other reasons. In order to account for off-target effects, some of the cytotoxicity assays were also carried out with HL-60 cells, which do not express ALDH1A enzymes (as seen in **Figure 4**). For most inhibitors tested, HL-60 cell death was observed at similar inhibitor concentrations and incubation times than those of A549 cells (data not shown). Thus these compounds are likely to display cytotoxicity due to other reasons apart from ALDH1A inhibition. Moreover, A549 cells express ALDH1A1 and ALDH1A3 (**Figure 4**), thus in the case of WIN 18,446, which is only able to inhibit ALDH1A2 (**Table 1**), toxicity may not be associated with the reduction of ALDH activity. According to results obtained with DEAB and compound **64**, which are able to inhibit mainly ALDH1A1 and ALDH1A3, respectively, *in vitro*, the relationship between ALDH inhibition and reduction of cell viability could be valid, but further experiments had to be carried out in order to check for this hypothesis. One of these experiments was the determination of the cytotoxic effect of retinaldehyde alone or in the presence of 100  $\mu$ M DEAB. Results are shown in **Figure 9**.

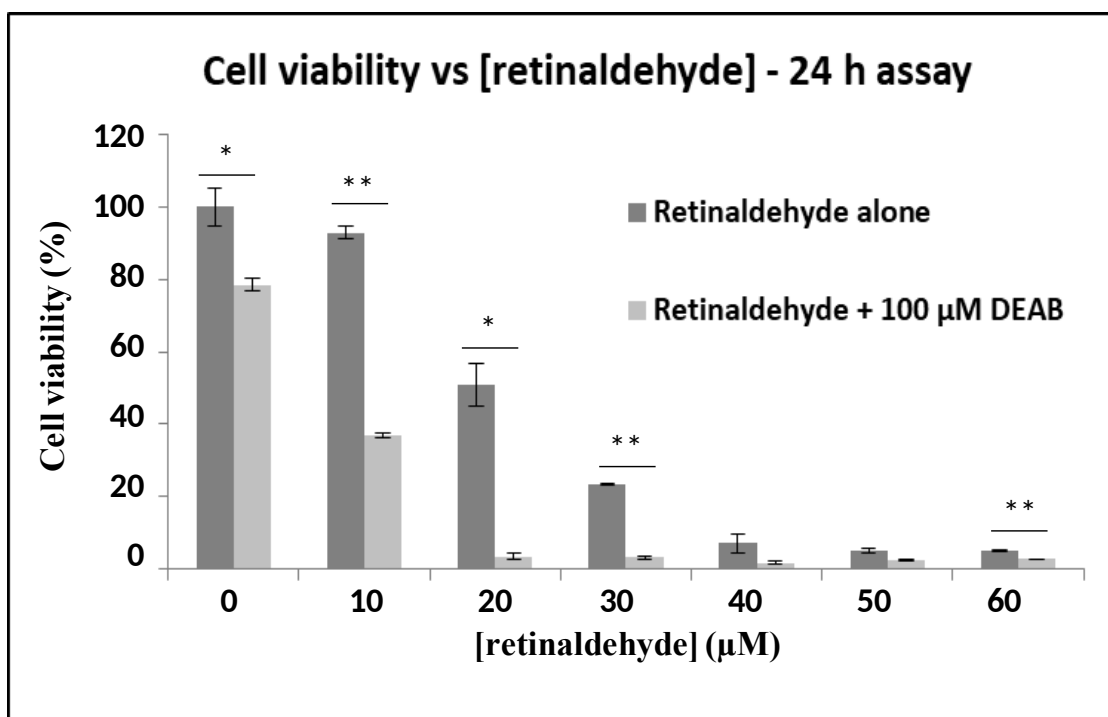


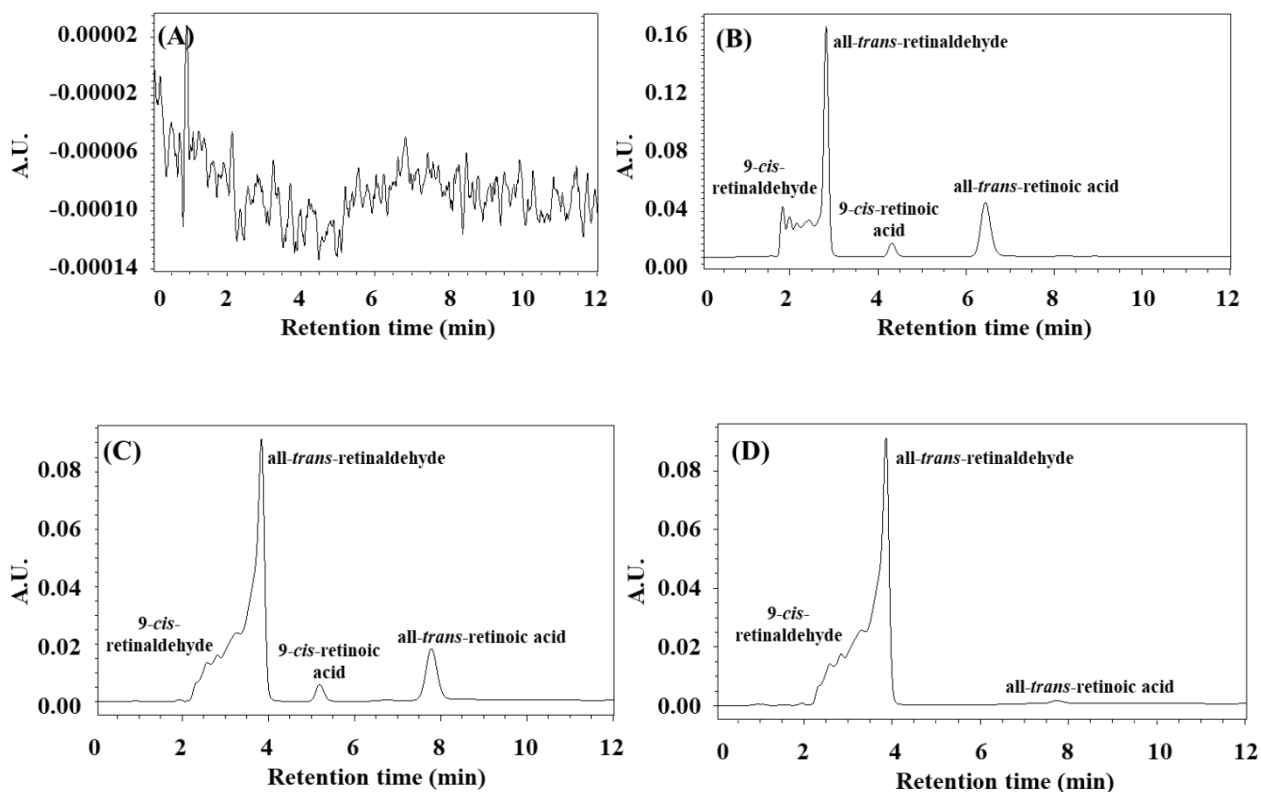
**Figure 9.** Bar diagram of A549 cell viability assays after 24-h treatment with retinaldehyde alone (dark grey bars) or in combination with 100 μM DEAB (light grey bars). Cell viability upon 24-h treatment with 100 μM DEAB alone decreased to 80%, as seen in **Figure 5A**. Data are the mean ± SE of percentage values relative to untreated controls (n = 3) from a single representative experiment. \* $p < 0.05$ , \*\* $p < 0.01$ , compared with untreated controls. (2-column fitting image)

Although retinaldehyde is the physiological substrate of ALDH1A enzymes, it can be seen in this experiment that it has an important cytotoxic effect on A549 cells at concentrations above 10 μM. Interestingly, cell mortality was potentiated when retinaldehyde was administered in combination with DEAB. This suggests that, in the absence of inhibitor, ALDH activity may be sufficient to eliminate retinaldehyde at moderate concentrations. However, when the inhibitor is concomitantly added, ALDH activity is blocked and retinaldehyde detoxification is hampered, leading to decreased cell viability. This result, supported by the previous work of Park *et al.* [18], seems to evidence that DEAB is able to diffuse inside the cells. This information was already known; in fact, the entrance of DEAB in the cells is one of the bases of the widely used Aldefluor™ assay, a common strategy to identify human cells expressing high levels of ALDH activity [19]. On the other hand, this result highlights the promising possibilities of using an

ALDH inhibitor, such as one of the compounds tested in this study, in combination with a carbonyl-based drug compound as a novel form of cancer therapy.

### 3.2.3. Inhibition of ALDH activity in A549 lung cancer cells

In order to link cell death with inhibition of ALDH activity, this inhibition has to be observed in cells when retinaldehyde is added together with the inhibitor. To this end, an HPLC-based method was used to measure the ALDH activity. After incubation and sample processing, retinaldehyde and retinoic acid could only be detected in the culture media, but not in cell extracts. HPLC chromatograms are depicted in **Figure 10**, and the calculated ALDH activities are shown in **Table 3**.



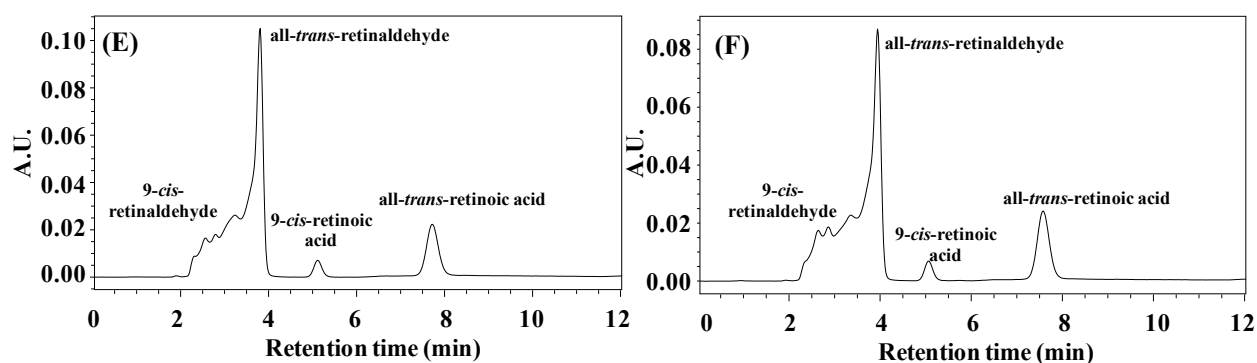


**Figure 10.** HPLC analysis of ALDH activity in A549 lung cancer cells. **(A)** Control without retinaldehyde and without inhibitor, **(B)** 30  $\mu$ M retinaldehyde without inhibitor (1-h treatment), **(C)** 30  $\mu$ M retinaldehyde with 10  $\mu$ M DEAB, **(D)** 30  $\mu$ M retinaldehyde with 100  $\mu$ M DEAB, **(E)** 30  $\mu$ M retinaldehyde with 10  $\mu$ M compound **64**, **(F)** 30  $\mu$ M retinaldehyde with 100  $\mu$ M compound **64**. (2-column fitting image)

As shown in **Figure 10A**, no retinoid peaks were detected when retinaldehyde was absent. In the presence of retinaldehyde without inhibitor, a major peak of all-*trans*-retinaldehyde appeared at approximately 3 min (**Figure 7B**). The left shoulder of the peak indicated the presence of retinaldehyde isomerization. The isomerization may have occurred during the incubation of the cells at 37°C for 1 h, despite the experiment was always carried out under dim red light. Due to the ALDH activity of the cells, retinaldehyde was transformed into all-*trans*-retinoic acid, which could be observed as a peak at 6.5 min, approximately. A minor peak, which could correspond to 9-*cis*-retinoic acid (likely derived from retinaldehyde isomerization) was also detected at nearly 4.5 min.

As a consequence of the addition of DEAB, the area under the peak corresponding to retinoic acid was reduced, whereas the area under the peak of retinaldehyde was increased, suggesting that DEAB entered the cells and inhibited the ALDH reaction. The effect of the inhibitor was visibly more obvious in the presence of 100  $\mu$ M DEAB (**Figure 10D**); in this case, the peak of product was much smaller than in the presence of 10  $\mu$ M DEAB (**Figure 10C**). The production of retinoic acid from retinaldehyde in A549 cells can only take place via ALDH1A1 and ALDH1A3 (**Figure 4**) and, as described above, DEAB is an excellent inhibitor of ALDH1A1 *in*

*vitro*, but not of ALDH1A3 (**Table 1**). HPLC results suggest that ALDH1A1 may be the main enzyme contributing to ALDH activity in A549 cells. This could explain that the ALDH activity was almost completely abolished in the presence of DEAB. The observed remaining activity (**Table 3**) could be due to ALDH1A3, which is not inhibited by DEAB.

When compound **64** was added to the cell cultures (**Figures 10E and F**), inhibition of the ALDH reaction also occurred. This statement may not be evident from the direct observation of the graphs, but is clear from the comparison of specific activities (**Table 3**), which take into account the total amount of protein, determined by the Bradford assay. What can be seen in the graphs is that the inhibition by compound **64** was not as potent as the inhibition with DEAB (the area under the retinaldehyde peak was lower than that of the peak obtained in the presence of DEAB, and the area under the product peak was greater). Interestingly, the specific activity calculated in the presence of both 10  $\mu$ M and 100  $\mu$ M compound **64** was the same (**Table 3**). Most likely, 10  $\mu$ M compound **64** was enough to completely inhibit ALDH1A3 activity, and the remaining activity was due to ALDH1A1, which is not inhibited by compound **64** (**Table 1**).

**Table 3.** Specific ALDH activity in A549 cells in the absence or presence of inhibitor.

	[Inhibitor]				
	0 $\mu$ M	10 $\mu$ M DEAB	100 $\mu$ M DEAB	10 $\mu$ M compound <b>64</b>	100 $\mu$ M compound <b>64</b>
<b>Specific ALDH activity (mU/mg)</b>	0.110	0.015	0.0008	0.033	0.033
<b>% of activity</b>	100%	14%	0.7%	29%	29%

ALDH activity was calculated from the amount of all-*trans*-retinoic acid produced as seen in the chromatograms shown in **Figure 10**. The activity was measured in A549 cells in the absence of inhibitor and in the presence of 10  $\mu$ M and 100  $\mu$ M DEAB or compound **64**, after incubation of the cells with 30  $\mu$ M retinaldehyde for 1 h. The percentage of activity with respect to the activity in the absence of inhibitor is indicated at each concentration of inhibitor. Data are the mean of triplicates.



#### 4. Conclusions

In this work, four synthetic compounds have been kinetically characterized *in vitro* as putative inhibitors of ALDH1A enzymes and tested as cytotoxic agents on human cancer cells.

From the *in vitro* characterization of the compounds with enzymes, we can conclude that: DEAB is the best inhibitor of ALDH1A1, specifically a competitive inhibitor showing  $K_i = 0.13 \mu\text{M}$  and  $\text{IC}_{50} = 0.18 \mu\text{M}$ ; although not as good as DEAB, compound **5a** is also a suitable inhibitor against ALDH1A1, with  $\text{IC}_{50} = 5.42 \mu\text{M}$ ; WIN 18,446 is the best inhibitor against ALDH1A2, specifically an irreversible inhibitor with  $\text{IC}_{50} = 0.07 \mu\text{M}$  (with an incubation time of 5 min); Compound **64** is the best inhibitor of ALDH1A3, displaying non-competitive inhibition with  $K_i = 1.77 \mu\text{M}$  and  $\text{IC}_{50} = 1.17 \mu\text{M}$ .

The studies on cancer cell lines confirmed firstly that A549 lung cancer cells express ALDH1A1 and ALDH1A3, but not ALDH1A2. Secondly, we observed that except for compound **5a**, all the inhibitors had a toxic effect on A549 cells at high concentrations of inhibitor. Specifically, compound **64** displayed the greater toxicity, especially 72 h after the addition of the inhibitor, reducing cell viability down to approximately 10%.

Retinaldehyde also had a toxic effect on A549 cells, which was increased when DEAB was concomitantly added. DEAB is thought to partially inhibit the ALDH1A activity in the cells, and thus, it hampers aldehyde elimination. Inhibition of the reaction in the cells by DEAB was evidenced by HPLC analysis, and it was also proved with compound **64**, which showed less inhibitory potency than DEAB.

Overall, the availability of the three purified ALDH1A enzymes allowed us to describe selective and potent inhibitors for each ALDH1A enzyme, some with novel scaffolds and showing cytotoxic activity against human cancer cells. Cytotoxicity was enhanced in the presence of toxic retinaldehyde and was related to the inhibitor blockade of ALDH activity. These results appear to be very promising in developing new strategies based on combination therapy approaches to counteract cancer cell chemoresistance.

## **Conflict of interest**

The authors declare that there are no conflicts of interest.

## **Acknowledgements**

This work was funded by the Spanish Ministerio de Economía y Competitividad (BFU2011-24176 and BIO2016-78057).. Partial financial support was provided by the Faculty of Pharmacy, Zagazig University (Egypt). We thank Dr. Maria Jolis, from the Department of Mathematics (UAB), for her guidance in performing statistical analyses.

## **Appendix A. Supplementary material**

**Table S1.** Antibodies used for Western blotting. **Figures S1-S4.** Sigmoidal plots obtained for inhibition against different ALDH1A enzymes. **Figures S5-S6.** Individual Michaelis-Menten plots of inhibition of ALDH1A enzymes in the presence of various concentrations of inhibitor.

## **References**

- [1] World Health Organization (WHO). Cancer. Accessed on 16<sup>th</sup> August 2018. Available online at: <http://www.who.int/en/news-room/fact-sheets/detail/cancer>.
- [2] I. Ma, A. Allan, The Role of Human Aldehyde Dehydrogenase in Normal and Cancer Stem Cells, *Stem Cell Rev. Reports* 7 (2011) 292–306.
- [3] J. Moreb, D. Ucar-Bilyeu, A. Khan, Use of retinoic acid/aldehyde dehydrogenase pathway as potential targeted therapy against cancer stem cells, *Cancer Chemother. Pharmacol.* 79 (2017) 295–301.

- [4] P. Marcato, C.A. Dean, C.A. Giacomantonio, P.W.K. Lee, Aldehyde dehydrogenase : its role as a cancer stem cell marker comes down to the specific isoform, *Cell Cycle* 10 (2011) 1378–1384.
- [5] V. Vasiliou, D.C. Thompson, C. Smith, M. Fujita, Y. Chen, Aldehyde dehydrogenases : From eye crystallins to metabolic disease and cancer stem cells, *Chem. Biol. Interact.* 202 (2013) 2–10.
- [6] X. Xu, S. Chai, P. Wang, C. Zhang, Y. Yang, Y. Yang, K. Wang, Aldehyde dehydrogenases and cancer stem cells, *Cancer Lett.* 369 (2015) 50–57.
- [7] V. Koppaka, D. Thompson, Y. Chen, M. Ellermann, K. Nicolaou, R. Juvonen, D. Petersen, R. Deitrich, T. Hurley, V. Vasiliou, Aldehyde Dehydrogenase Inhibitors : a Comprehensive Review of the Pharmacology, Mechanism of Action, Substrate Specificity, and Clinical Application, *Am. Soc. Pharmacol. Exp. Ther.* 64 (2012) 520–539.
- [8] C.A. Morgan, T.D. Hurley, Characterization of two distinct structural classes of selective aldehyde dehydrogenase 1A1 inhibitors, *J. Med. Chem.* 58 (2015) 1964–1975.
- [9] K. Metwally, H. Pratsinis, D. Kletsas, L. Quattrini, V. Coviello, C.L. Motta, A.A. El-Rashedy, M.E. Soliman, Novel quinazolinone-based 2,4-thiazolidinedione-3-acetic acid derivatives as potent aldose reductase inhibitors, *Future Med. Chem.* 9 (2017) 2147–2166.
- [10] I. Crespo, J. Giménez-Dejoz, S. Porté, A. Cousido-Siah, A. Mitschler, A. Podjarny, H. Pratsinis, D. Klestas, X. Parés, F.X. Ruiz, K. Metwally, J. Farrés, Design, synthesis, structure-activity relationships and X-ray structural studies of novel 1-oxopyrimido [4,5-*c*] quinoline-2-acetic acid derivatives as selective and potent inhibitors of human aldose reductase, *Eur. J. Med. Chem.* 152 (2018) 160–174.
- [11] M. Domínguez, R. Pequerul, R. Alvarez, J. Giménez-Dejoz, E. Birta, S. Porté, R. Rühl,

- X. Parés, J. Farrés, A.R. de Lera, Synthesis of apocarotenoids by acyclic cross metathesis and characterization as substrates for human retinaldehyde dehydrogenases, *Tetrahedron* 74 (2018) 2567–2574.
- [12] S. Sołobodowska, J. Giebułtowicz, R. Wolinowska, P. Wroczyński, Contribution of ALDH1A1 isozyme to detoxification of aldehydes present in food products, *Acta Pol. Pharm.* 69 (2012) 1380–1383.
- [13] M.A. Kane, N. Chen, S. Sparks, J.L. Napoli, Quantification of endogenous retinoic acid in limited biological samples by LC / MS / MS, *Biochem. J.* 388 (2005) 363–369.
- [14] C. Morgan, B. Parajuli, C. Buchman, K. Dria, T. Hurley, N,N-diethylaminobenzaldehyde (DEAB) as a substrate and mechanism-based inhibitor for human ALDH isoenzymes, *Chem. Biol. Interact.* 234 (2016) 18–28.
- [15] J. Paik, M. Haenisch, C.H. Muller, A.S. Goldstein, S. Arnold, N. Isoherranen, T. Brabb, P.M. Treuting, J.K. Amory, Inhibition of retinoic acid biosynthesis by the bisdichloroacetyldiamine WIN 18 , 446 markedly suppresses spermatogenesis and alters retinoid metabolism in mice, *J. Biol. Chem.* 289 (2014) 15104–15117.
- [16] Y. Chen, J. Zhu, K.H. Hong, D.C. Mikles, G.I. Georg, A.S. Goldstein, J.K. Amory, E. Schönbrunn, Structural Basis of ALDH1A2 Inhibition by Irreversible and Reversible Small Molecule Inhibitors, *ACS Chem. Biol.* 13 (2018) 582–590.
- [17] R.A. Copeland, A.J. Wiley, "Reversible inhibitors", *Enzymes: a practical introduction to structure, mechanism, and data analysis*, Second Edition, Wiley-VCH, New York, 2000, 266-304.
- [18] J. Park, K. Jung, J. Lee, S. Moon, Y. Cho, K. Lee, Inhibition of aldehyde dehydrogenase 1 enhances the cytotoxic effect of retinaldehyde on A549 cancer cells, *Oncotarget* 8 (2017) 99382–99393.
- [19] R. Storms, A. Trujillo, J. Springer, L. Shah, O. Colvin, S. Ludeman, C. Smith, Isolation

of primitive human hematopoietic progenitors on the basis of aldehyde dehydrogenase activity, *Proc. Natl. Acad. Sci. U. S. A.* 96 (1999) 9118–9123.

## Supplementary material

**Table S1.** Antibodies used for Western blotting.

	Antibodies		Provider	Host	Dilution
<b>Western blot ALDH1A1</b>	Primary antibody	Monoclonal anti-ALDH1A1	R&D Systems	Mouse	1:500
	Secondary antibody	Anti-mouse IgG (H+L)-HRP conjugate	Bio-Rad	Goat	1:4000
<b>Western blot ALDH1A2</b>	Primary antibody	Polyclonal anti-ALDH1A2	Abcam	Rabbit	1:500
	Secondary antibody	ECL <sup>TM</sup> Anti-rabbit IgG HRP-linked whole antibody	GE Healthcare Life Sciences	Donkey	1:4000
<b>Western blot ALDH1A3</b>	Primary antibody	Polyclonal anti-ALDH1A3	GeneTex	Rabbit	1:2000
	Secondary antibody	ECL <sup>TM</sup> Anti-rabbit IgG HRP-linked whole antibody	GE Healthcare Life Sciences	Donkey	1:4000

The antibodies used in each Western blot experiment are indicated in this Table. A brief description of the antibody, the provider, the host and the implemented dilution are indicated.

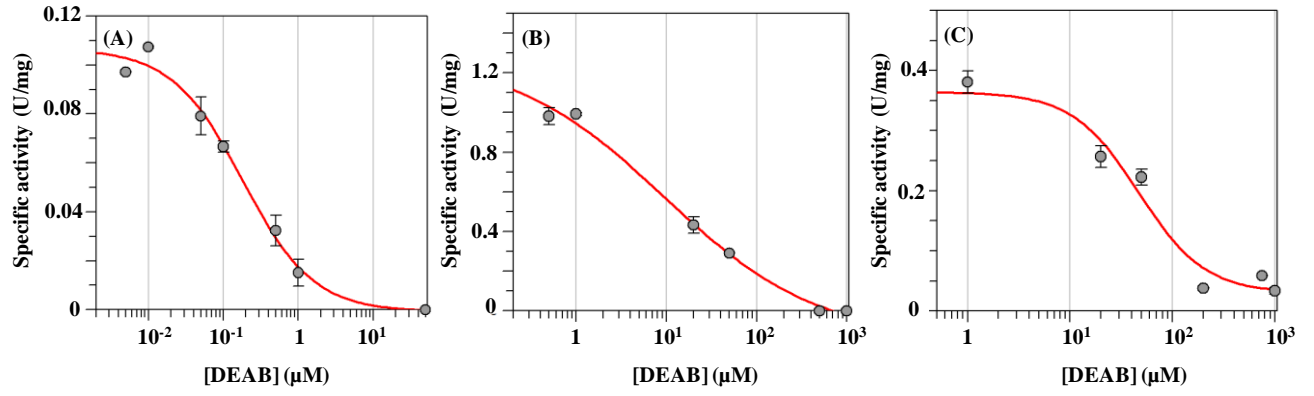


**Figure S1.** Sigmoidal plots obtained for DEAB inhibition against (A) ALDH1A1 ( $IC_{50} = 0.18 \pm 0.05 \mu M$ ), (B) ALDH1A2 ( $IC_{50} = 10 \pm 3 \mu M$ ), and (C) ALDH1A3 ( $IC_{50} = 47 \pm 17 \mu M$ ). Data are the mean  $\pm$  SE of duplicate experiments.

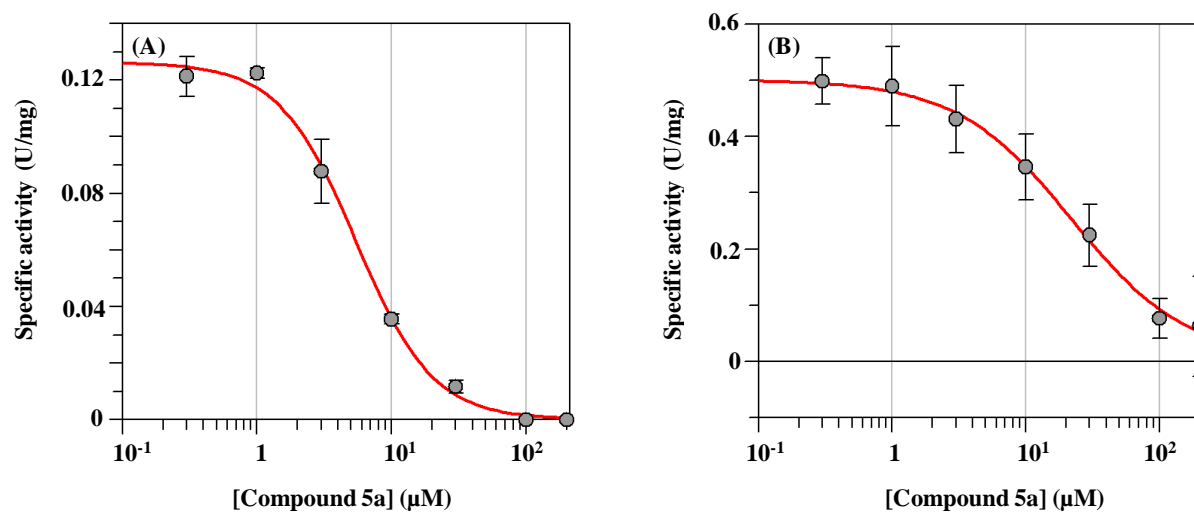


**Figure S2.** Sigmoidal plots obtained for compound **5a** inhibition against **(A)** ALDH1A1 ( $\text{IC}_{50} = 5.42 \pm 0.45 \mu\text{M}$ ), and **(B)** ALDH1A3 ( $\text{IC}_{50} = 23 \pm 4 \mu\text{M}$ ). Data are the mean  $\pm$  SE of duplicate experiments.



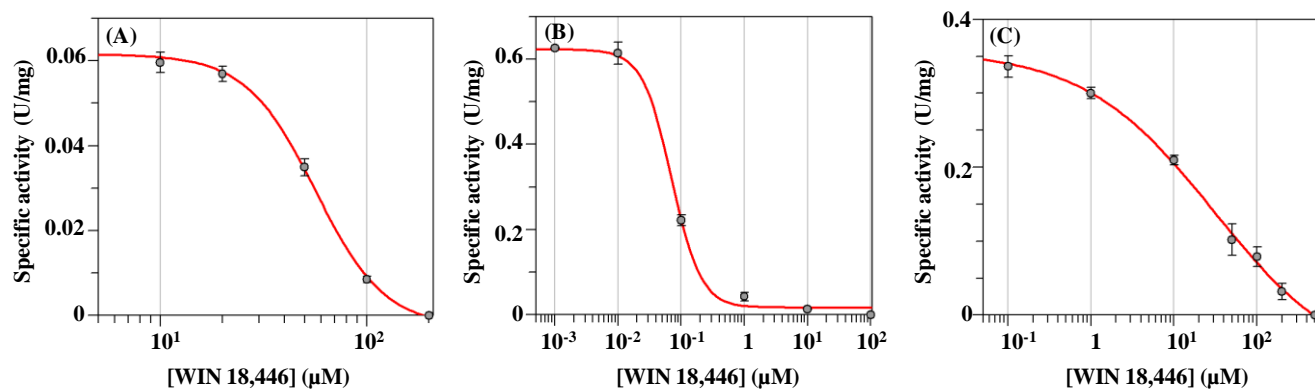


**Figure S3.** Sigmoidal plots obtained for WIN 18,446 inhibition against (A) ALDH1A1 (IC<sub>50</sub> = 56 ± 3 μM), (B) ALDH1A2 (IC<sub>50</sub> = 0.07 ± 0.01 μM), and (C) ALDH1A3 (IC<sub>50</sub> = 31 ± 8 μM).

Data are the mean ± SE of duplicate experiments.

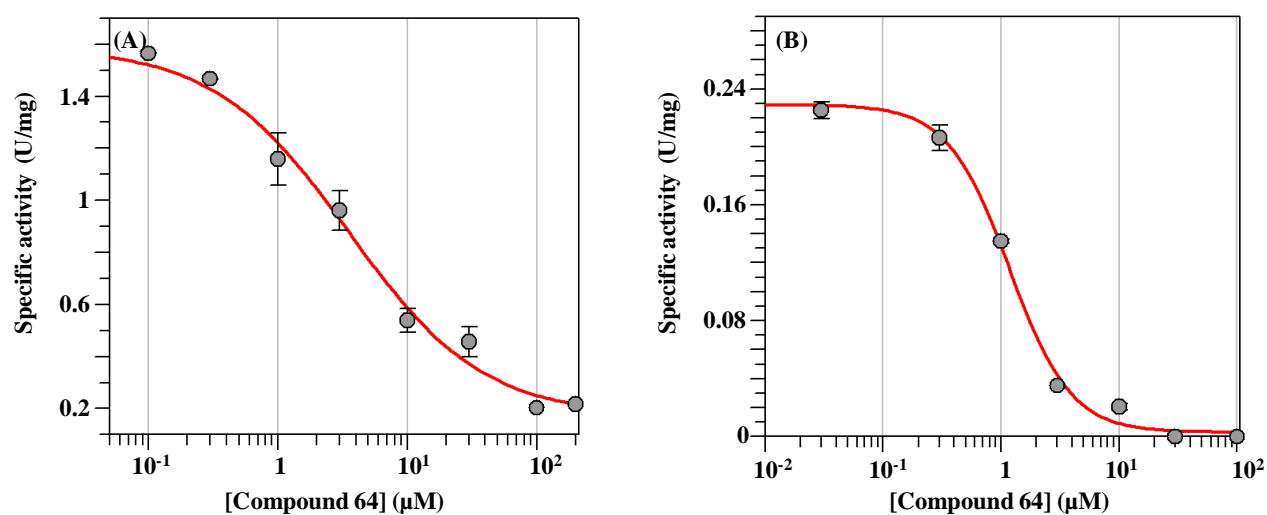


**Figure S4.** Sigmoidal plots obtained for compound **64** inhibition against **(A)** ALDH1A2 ( $\text{IC}_{50} = 3.50 \pm 0.80 \mu\text{M}$ ), and **(B)** ALDH1A3 ( $\text{IC}_{50} = 1.17 \pm 0.11 \mu\text{M}$ ). Data are the mean  $\pm$  SE of duplicate experiments.

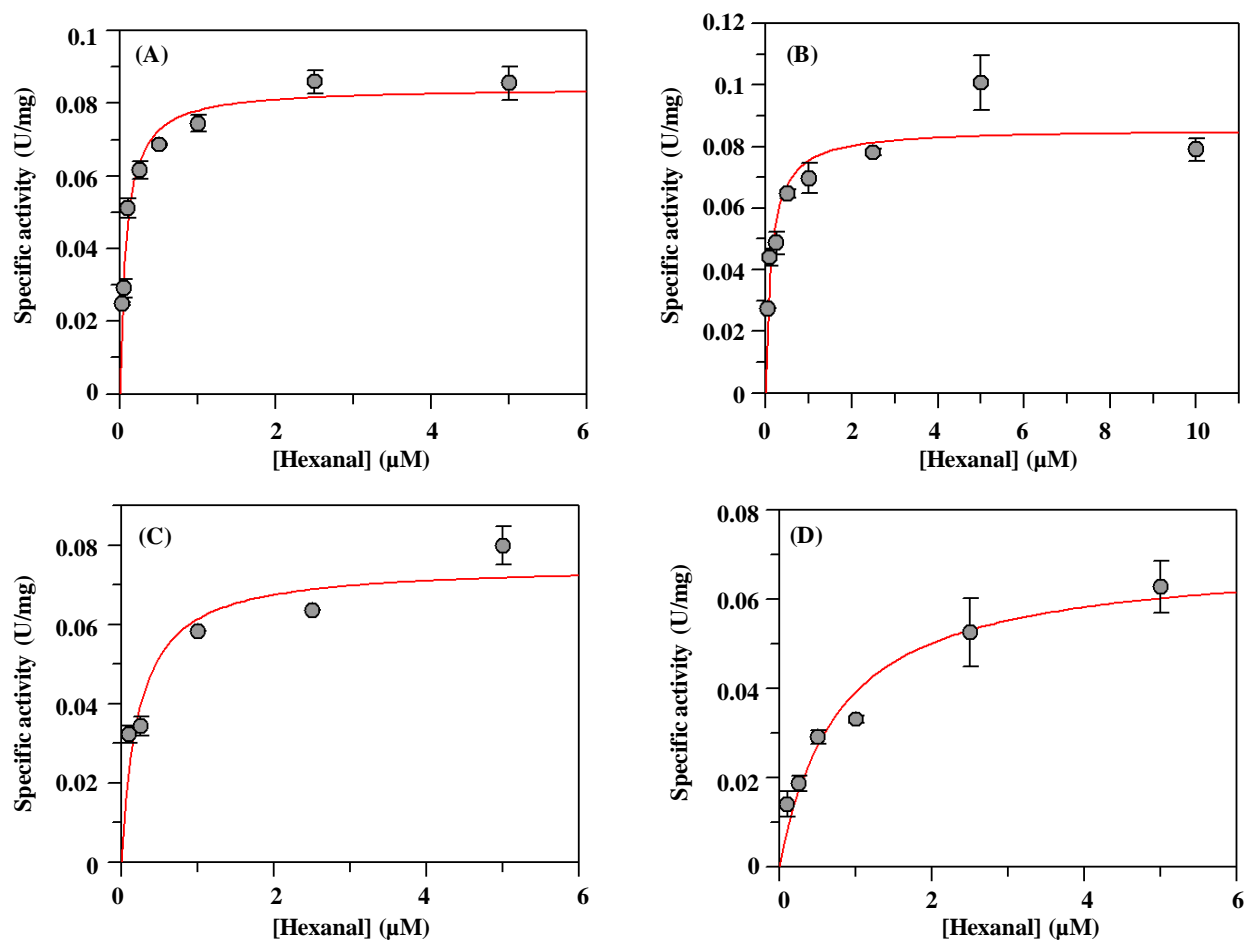


**Figure S5.** Individual Michaelis-Menten plots of ALDH1A1 inhibition in the presence of various concentrations of DEAB. **(A)** 0 μM ( $V_{max} = 0.084 \pm 0.003$  U/mg,  $K_m = 0.079 \pm 0.012$  μM), **(B)** 0.02 μM ( $V_{max} = 0.086 \pm 0.005$  U/mg,  $K_m = 0.133 \pm 0.041$  μM), **(C)** 0.2 μM ( $V_{max} = 0.075 \pm 0.007$  U/mg,  $K_m = 0.220 \pm 0.090$  μM), **(D)** 2 μM ( $V_{max} = 0.069 \pm 0.006$  U/mg,  $K_m = 0.769 \pm 0.204$  μM). Hexanal was used as the substrate of the reaction. Data are the mean  $\pm$  SE of duplicate experiments.

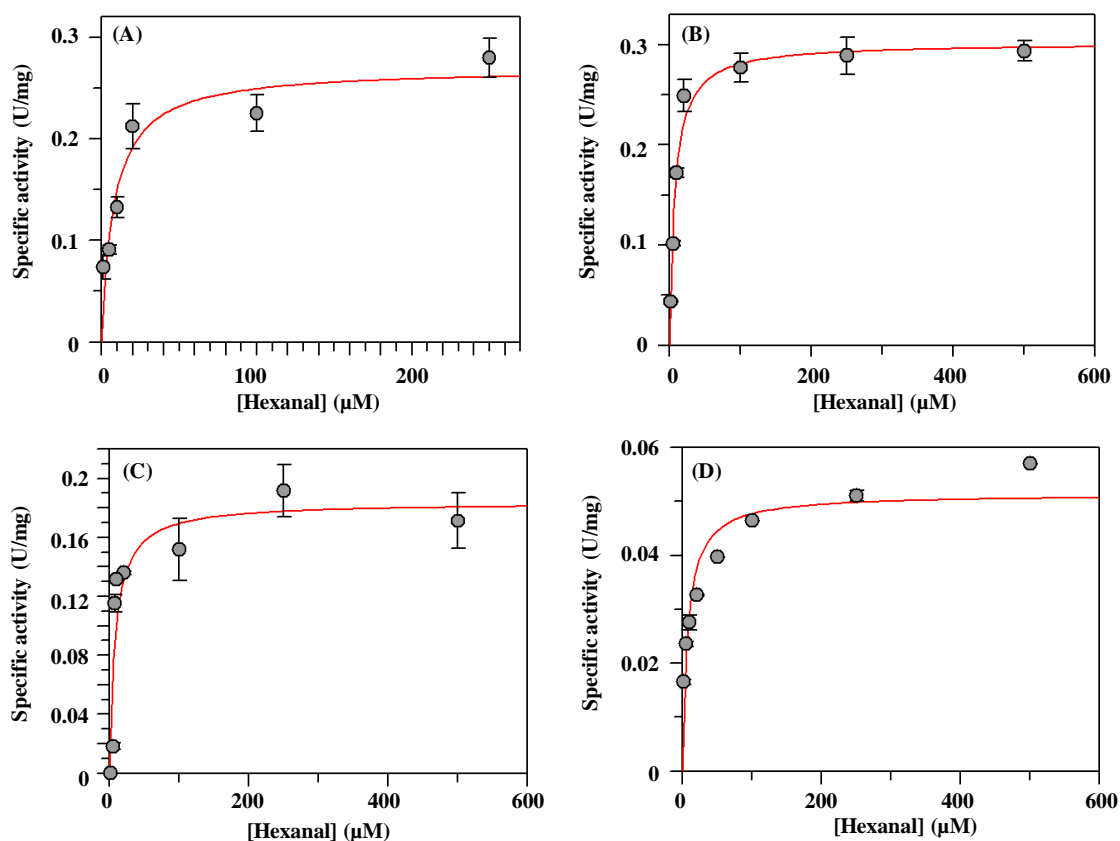


**Figure S6.** Individual Michaelis-Menten plots of ALDH1A3 inhibition in the presence of various concentrations of compound **64**. (A) 0 μM ( $V_{max} = 0.269 \pm 0.025$  U/mg,  $K_m = 8 \pm 3$  μM), (B) 0.1 μM ( $V_{max} = 0.301 \pm 0.011$  U/mg,  $K_m = 7 \pm 1$  μM), (C) 1 μM ( $V_{max} = 0.184 \pm 0.019$  U/mg,  $K_m = 8 \pm 3$  μM), (D) 10 μM ( $V_{max} = 0.0519 \pm 0.004$  U/mg,  $K_m = 8 \pm 3$  μM). Hexanal was used as the substrate of the reaction. Data are the mean  $\pm$  SE of duplicate experiments.